Received: 27 August 2021 | Accepted: 1 October 2021

DOI: 10.1111/1759-7714.14191

ORIGINAL ARTICLE

WILEY

Circ_0016760 accelerates non-small-cell lung cancer progression through miR-646/AKT3 signaling in vivo and in vitro

Shan Chen[1] | **Long Zhou**[2] | **Ruizhi Ran**[1] | **Jinqi Huang**[3] | **Yong Zheng**[3] | **Maohui Xing**[1] | **Yanli Cai**[3]

[1]Department of Oncology, The Central Hospital of Enshi Tujia and Miao Autonomous Prefecture, Enshi, China

[2]Department of Pulmonary and Critical Care Medicine, The Central Hospital of Enshi Tujia and Miao Autonomous Prefecture, Enshi, China

[3]Department of Cardiothoracic Surgery, The Central Hospital of Enshi Tujia and Miao Autonomous Prefecture, Enshi, China

Correspondence
Yanli Cai, Department of Cardiothoracic Surgery, The Central Hospital of Enshi Tujia and Miao Autonomous Prefecture, No. 158 Wuyang Avenue, Enshi, 445000, China.
Email: yanlicaicn@163.com

Abstract

Background: Currently, the prognosis of non-small-cell lung cancer (NSCLC) patients remains dismal due to recurrence and metastasis. The purpose of our study was to explore the role of circular RNA_0016760 (circ_0016760) in NSCLC progression and its associated mechanism.

Methods: Quantitative real-time polymerase chain reaction (qRT-PCR) was implemented to measure the expression of circ_0016760, microRNA-646 (miR-646) and AK strain thymoma serine/threonine kinase 3 (AKT3). The protein level of AKT3 was examined by Western blot assay. Cell Counting Kit 8 assay, transwell assays, and flow cytometry were conducted to analyze cell proliferation, metastasis, and apoptosis. Dual-luciferase reporter assay was used to confirm the interactions that were predicted by bioinformatics software (Circular RNA Interactome and TargetScan). A xenograft tumor model was built to investigate the role of circ_0016760 in vivo.

Results: Circ_0016760 and AKT3 were highly expressed in NSCLC tissue specimens and cell lines. Circ_0016760 interference suppressed cell proliferation, migration, and invasion and promoted the apoptosis of NSCLC cells. Circ_0016760 interacted with miR-646 and negatively regulated its expression. MiR-646 silencing partly counteracted circ_0016760 knockdown-mediated influences in NSCLC cells. MiR-646 bound to the AKT3 3′ untranslated region in NSCLC cells, and miR-646 overexpression-induced effects in NSCLC cells were partly overturned by the addition of AKT3 overexpression plasmid. Circ_0016760 silencing reduced the expression of AKT3 through enhancing miR-646 expression. Circ_0016760 knockdown suppressed NSCLC tumor growth in vivo.

Conclusion: Circ_0016760 played an oncogenic role to promote the proliferation, migration, and invasion and restrained the apoptosis of NSCLC cells via miR-646/AKT3 signaling.

KEYWORDS
AKT3, circ_0016760, miR-646, non-small-cell lung cancer

INTRODUCTION

Non-small-cell lung cancer (NSCLC) is the most common pathological subtype of lung cancer.[1] Although considerable improvement has been made in the clinical diagnosis and treatment of NSCLC, the prognosis of NSCLC patients remains unsatisfactory owing to recurrence and distant metastasis.[2–4] Understanding the molecular mechanism behind NSCLC progression is meaningful for identifying novel effective therapeutic targets.

Shan Chen and Long Zhou contributed equally to this work.

Circular RNAs (circRNAs) are a class of noncoding RNAs (ncRNAs) featuring a covalently continuous circular structure without 3′ or 5′ ends.[5,6] Accumulating studies have demonstrated the involvement of circRNAs in tumorigenesis. For example, circ-DNMT1 is reported to accelerate the development of breast cancer by promoting autophagy.[7] Circ_0026344 is reported to inhibit the motility of colorectal cancer cells.[8] A previous study reported that circ_0016760 expression is upregulated in NSCLC and circ_0016760 plays an oncogenic role in NSCLC.[9] However, the mechanism of circ_0016760 in biological properties of NSCLC cells has not been fully addressed.

MicroRNAs (miRNAs) are another group of noncoding RNAs that are 18–24 nucleotides in length.[10] miRNAs are reported to play pivotal regulatory roles in cancer initiation and progression.[11,12] Accumulating evidence has demonstrated that circRNAs can function as miRNA sponges to regulate cellular biological phenotypes.[13] For instance, circ-ABCB10 is reported to facilitate the malignant behaviors of breast cancer cells by targeting miR-1271.[14] Circ_0078767 is reported to restrain NSCLC development by acting as a molecular sponge for miR-330-3p.[15] Through bioinformatics analysis, miR-646 was predicted as a candidate target of circ_0016760 in this study. Previous studies demonstrated that miR-646 plays a tumor suppressor role in many malignancies,[16–19] including NSCLC. For instance, Wang et al. claimed that miR-646 restrains the malignant behaviors of NSCLC cells by downregulating FGF2 and CCND2.[19] In this study, the interaction between miR-646 and circ_0016760, and their functional correlation in NSCLC progression were explored.

It is widely established that miRNAs are involved in the regulation of cellular physiological and pathological processes by interacting with the 3′ untranslated region (3′ UTR) of messenger RNAs (mRNAs), thereby causing translational repression or degradation of target mRNAs.[20,21] Through bioinformatics analysis, AK strain thymoma serine/threonine kinase 3 (AKT3) was predicted as a possible target of miR-646 in this study. AKT3 is reported to play an oncogenic role in many malignancies. For instance, miR-16-5p is reported to suppress the development of breast cancer by downregulating AKT3, thus inactivating NF-κB signaling.[22] LINC00565 is reported to facilitate the proliferation while blocking the apoptosis of gastric cancer cells by enhancing AKT3 expression via sponging miR-665.[23] As for NSCLC, Qi et al. claimed that miR-217 attenuates NSCLC development by downregulating AKT3,[24] indicating the pro-tumor role of AKT3 in NSCLC. In the current study, the binding relation between miR-646 and AKT3, and their functional association in NSCLC progression were investigated.

In this study, we first analyzed the expression pattern of circ_0016760 in NSCLC tissues and cell lines. Loss-of-function experiments were conducted to analyze the biological role of circ_0016760 in NSCLC cells. Then, the downstream miRNA/mRNA axis of circ_0016760 was predicted by bioinformatics analysis and verified by rescue experiments.

MATERIALS AND METHODS

Clinical samples

Fifty pairs of NSCLC tissues and adjacent normal tissues were obtained from patients who had been diagnosed with NSCLC and underwent surgical resection at the Central Hospital of Enshi Tujia and Miao Autonomous Prefecture. All samples were stored at −80°C until the determination of RNA or protein expression. All participants gave informed consent. The protocol for the clinical experiments was approved by the Ethics Committee of the Central Hospital of Enshi Tujia and Miao Autonomous Prefecture. Clinical experiments were performed in accordance with the Declaration of Helsinki.

Cell culture

Human normal bronchial epithelial cell line 16HBE and two NSCLC cell lines (A549 and H460) were purchased from the Cell Resource Center of the Shanghai Institute of Biochemistry (Shanghai, China). All the above-mentioned cell lines were grown aat the Roswell Park Memorial Institute-1640 medium (RPMI-1640; Gibco) plus 10% fetal bovine serum (FBS; Gibco) and 1% penicillin/streptomycin (Sangon Biotech). All cell lines were maintained at 37°C atmosphere with 5% CO_2.

Cyclization validation

RNA samples (2 μg) were incubated with 3 U/μg RNase R (Epicenter Technologies) for 30 min at 37°C. The levels of circ_0016760 and SNAP47 mRNA were determined by quantitative real-time polymerase chain reaction (qRT-PCR).

Subcellular fractionation

NSCLC cells were washed using phosphate buffered saline (PBS) and re-suspended. PARIS™ Kit Protein and RNA Isolation system (Thermo Fisher Scientific) were utilized to extract cytoplasmic RNA and nuclear RNA.

Quantitative reverse transcription polymerase chain reaction

RNA was extracted with TRIzol (Invitrogen). RNA was used as the template to synthesize cDNA using a Prime Script RT reagent Kit (for circ_0016760, SNAP47 and AKT3; Takara)

TABLE 1 Primers used in qRT-PCR

Gene	Direction	Sequence
Circ_0016760	Forward primer	5′-CTCAGAAGCGCAAGAACCTC-3′
	Reverse primer	5′-TGGGCTCCAGGTAGTAGGTG-3′
SNAP47	Forward primer	5′-GCCGGATTTGAAGAGGCAGAAG-3′
	Reverse primer	5′-ATCTCTCCAGTGCTGTCAGTC-3′
MiR-646	Forward primer	5′-GGCGAAGCAGCTGCCTC-3′
	Reverse primer	5′-GCAGGGTCCGAGGTATTC-3′
AKT3	Forward primer	5′-TTTTCTCTATTATTTGGGCTGAGTC-3′
	Reverse primer	5′-CCCCTCTTCTGAACCCAACC-3′
U6	Forward primer	5′-CTCGCTTCGGCAGCACA-3′
	Reverse primer	5′-AACGCTTCACGAATTTGCGT-3′
GAPDH	Forward primer	5′-TATGATGACATCAAGAAGGTGGT-3′
	Reverse primer	5′-TGTAGCCAAATTCGTTGTCATAC-3′

and a One Step Prime Script miRNA cDNA Synthesis Kit (for miR-646; Takara). The synthesized cDNA was used as the template for the PCR, which was conducted using SYBR Premix Ex Taq II (Takara) and specific primers shown in Table 1. PCR was conducted on an ABI 7500 HT system (Applied Biosystems). Glyceraldehyde-3-phosphate dehydrogenase (GAPDH) served as the control for circ_0016760, SNAP47, and AKT3 mRNA, while U6 acted as the internal reference for miR-646. The relative expression was analyzed by the $2^{-\Delta\Delta Ct}$ method.

Western blot assay

After isolating the protein content using radioimmunoprecipitation assay (RIPA) lysis buffer (Sangon Biotech), a BCA Kit (Beyotime) was used for protein quantification. Protein samples (35 μg) were loaded onto each well of the sodium dodecyl sulfate polyacrylamide gel electrophoresis (SDS-PAGE) gel to separate total proteins according to molecular weight and charge. Through semidry electrotransferring, these proteins were blotted to the polyvinylidene fluoride (PVDF) membrane (Bio-Rad). After sealing the nonspecific sites with 5% skimmed milk, primary antibodies, including anti-AKT3 (ab152157; Abcam) and anti-GAPDH (ab8245; Abcam), were incubated with the membrane with gentle agitation. Subsequently, horseradish peroxidase (HRP)-labeled secondary antibody (Abcam) was used to probe the membrane. Protein bands were visualized by a BeyoECL Plus Kit (Beyotime).

Cell transfection

Circ_0016760 targeting small interfering RNAs (si-circ_0016760#1, si-circ_0016760#2, and si-circ_0016760#3), AKT3 siRNA (si-AKT3), negative control siRNA (si-NC), circ_0016760 overexpression reconstructed plasmid (circ_0016760), pLCDH-cir empty vector (Vector), lentivirus short hairpin RNA against circ_0016760 (Lv-sh-circ_0016760), Lv-sh-NC, miR-646 mimics (miR-646), miR-NC, miR-646 inhibitor (in-miR-646), in-miR-NC, AKT3 reconstructed plasmid (pcDNA-AKT3), and pcDNA-control were purchased from GenePharma and Ribobio. The small RNA or plasmid was transfected into NSCLC cells with Lipofectamine 3000 reagent (Invitrogen) when cell confluence reached about 70%.

Cell Counting Kit 8 assay

NSCLC cells in 96-well plates were cultured to settle down. At an appropriate time after transfection (0 h, 24 h, 48 h or 72 h), 10 μl of Cell Counting Kit 8 (CCK8) reagent (Dojindo) was added to incubate with the transfected NSCLC cells for 2 h. The absorbance was determined at 450 nm. The cell proliferation curve was generated through continuously measuring the optical density.

Transwell assays

The migration and invasion abilities were measured using 24-well transwell chambers with a pore size of 8 μM (BD Biosciences) that was pre-coated with Matrigel (for transwell invasion assay; BD Biosciences) or not (for transwell migration assay). After transfection for 24 h, cells with serum-free medium were seeded into the upper chambers. The lower chambers were added with culture medium with 10% FBS. After 24 h of incubation, cells located in the upper surface were mechanically removed using the cotton swab. The numbers of migrated and invaded cells in five fields at a magnification time of 100 were counted under an optical microscope.

Flow cytometry

Annexin V-fluorescein isothiocyanate (Annexin V-FITC) Apoptosis Detection Kit (BD Biosciences) was used to analyze the proportion of NSCLC cells with $FITC^{+}$ and propidium $iodide^{+/-}$ ($PI^{+/-}$). NSCLC cells after 72 h of transfection were incubated with Annexin V-FITC (5 μl) and PI (5 μl) for 15 min in the dark. Cell apoptosis was assessed on FACSCalibur (BD Biosciences).

Target prediction

The miRNA binding partners of circ_0016760 were predicted by Circular RNA Interactome, and

TargetScan software was used to seek the mRNA targets of miR-646.

Dual-luciferase reporter assay

The sequence fragment of circ_0016760 or AKT3 3′UTR, including the putative complementary sites with miR-646, was synthesized and cloned into pmirGLO vector (Promega), termed wild-type circ_0016760 (WT-circ_0016760) and WT-AKT3. The mutant sequence fragment in circ_0016760 or AKT3 3′UTR was also amplified and inserted into pmirGLO vector (Promega) to construct MUT-circ_0016760 and MUT-AKT3. These luciferase plasmids were simultaneously transfected with miR-NC or miR-646 into NSCLC cells that were seeded in 24-well plates. The intensities of Firefly and Renilla luciferase were examined with the Dual-Luciferase Reporter Assay System Kit (Promega).

Xenograft tumor model

Animal manipulates were conducted according to the protocols approved by the Animal Care and Use Committee of the Central Hospital of Enshi Tujia and Miao Autonomous Prefecture and in accordance of guidelines provided by the National Institutes of Health Guide for the Care and Use of Laboratory Animals. BALB/c mice purchased from Vital River Laboratory Animal Technology (Beijing, China) were grouped into control group (Lv-sh-NC, $n = 5$) and silencing group (Lv-sh-circ_0016760, $n = 5$). A total of 2.7×10^6 A549 cells stably expressing Lv-sh-NC or Lv-sh-circ_0016760 were subcutaneously injected into the mice. Tumor growth was recorded through measuring the length and width of tumors every 4 days, and tumor volume was analyzed as width^2 × length × 0.5. At 28 days after inoculation, tumors were collected and weighed. qRT-PCR and Western blot assay were used to measure the expression of circ_0016760, miR-646, and AKT3 in tumor tissues.

Statistical analysis

Statistical analysis was conducted using GraphPad Prism 7.0 software and the data from three independent experiments were expressed as mean ± standard deviation. Differences in two groups or multiple groups were analyzed by Student's *t*-test or one-way analysis of variance (ANOVA) followed by Tukey's test, respectively. Linear correlation was analyzed by Spearman's correlation coefficient. The difference was identified to be statistically significant with $p < 0.05$.

RESULTS

The expression of circ_0016760 and AKT3 is aberrantly increased in NSCLC tissues and cell lines

We initially determined the expression of circ_0016760 in NSCLC tumor samples and cell lines along with adjacent

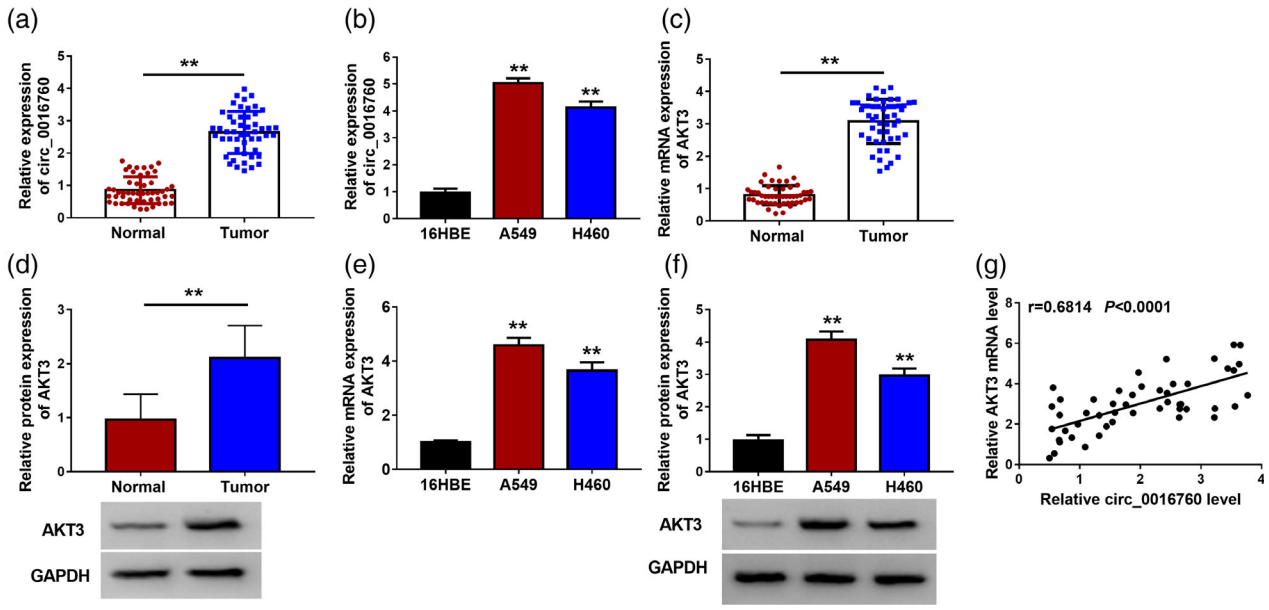

FIGURE 1 The expression of circ_0016760 and AKT3 is aberrantly increased in NSCLC tissues and cell lines. (a) Circ_0016760 expression was analyzed in 50 pairs of NSCLC tissues and adjacent nontumor tissues via qRT-PCR. (b) The expression pattern of circ_0016760 in normal human bronchial epithelial cell line 16HBE and two NSCLC cell lines (A549 and H460) was determined by qRT-PCR. (c) The mRNA level of AKT3 in 50 pairs of NSCLC tumor tissues and adjacent normal tissues was measured via qRT-PCR. (d) The abundance of AKT3 protein in NSCLC tumor tissues and adjacent normal specimens was detected by Western blot assay. (e) qRT-PCR was conducted to determine the mRNA expression of AKT3 in normal bronchial epithelial cell line 16HBE and NSCLC cell lines A549 and H460. (f) Western blot assay was utilized to measure the protein level of AKT3 in 16HBE and NSCLC cell lines. (g) Spearman's correlation coefficient was used to evaluate the linear correlation relationship between the expression of circ_0016760 and AKT3 mRNA level. $^{**}p < 0.01$

nontumor samples, and normal human bronchial epithelial cell line 16HBE. Circ_0016760 expression was observed to be remarkably upregulated in NSCLC tissues compared to adjacent normal tissues (Figure 1a). Circ_0016760 expression was also found to be enhanced in two NSCLC cell lines in comparison with that in the 16HBE cell line (Figure 1b). The circular structure of circ_0016760 was tested by exonuclease RNase R. RNase R digestion notably reduced the mRNA level of the linear form of circ_0016760 (SNAP47), while the level of circ_0016760 remained unaffected in Mock group and RNase R group (Figure S1a,b), suggesting that circ_0016760 was a circular transcript. The subcellular distribution of circ_0016760 in NSCLC cells was analyzed prior to exploring its biological function. Circ_0016760 was mainly located in the cytoplasmic fraction of NSCLC cells (Figure S1c,d), which implied that circ_0016760 might function as an miRNA sponge in NSCLC cells. Similar to the expression tendency of circ_0016760, AKT3 mRNA and protein expression were also elevated in NSCLC tumor tissues compared to adjacent nontumor tissues (Figure 1c,d). The mRNA and protein levels of AKT3 were upregulated in both NSCLC cell lines than that in 16HBE cell line (Figure 1e,f). AKT3 mRNA expression was positively correlated with the level of circ_0016760 (Figure 1g). These findings suggest that circ_0016760 and AKT3 might be implicated in the pathogenesis of NSCLC.

Circ_0016760 silencing hampers cell proliferation, migration, and invasion and triggers cell apoptosis in NSCLC cells

To explore the function of circ_0016760, we designed three siRNAs targeting its junction site to specifically knockdown circ_0016760 rather than its linear mRNA. Si-circ_0016760#2 was selected in the following experiments due to it high interference efficiency in both the two NSCLC cell lines (Figure 2a, b). We also tested the specificity of si-circ_0016760#2 in NSCLC cells. Transfection with si-circ_0016760#2 markedly reduced the expression of circ_0016760, while the expression of its linear counterpart (SNAP47 mRNA) remained almost unchanged with the transfection of si-NC or si-circ_0016760#2 (Figure S1e,f). Cell proliferation was markedly restrained with

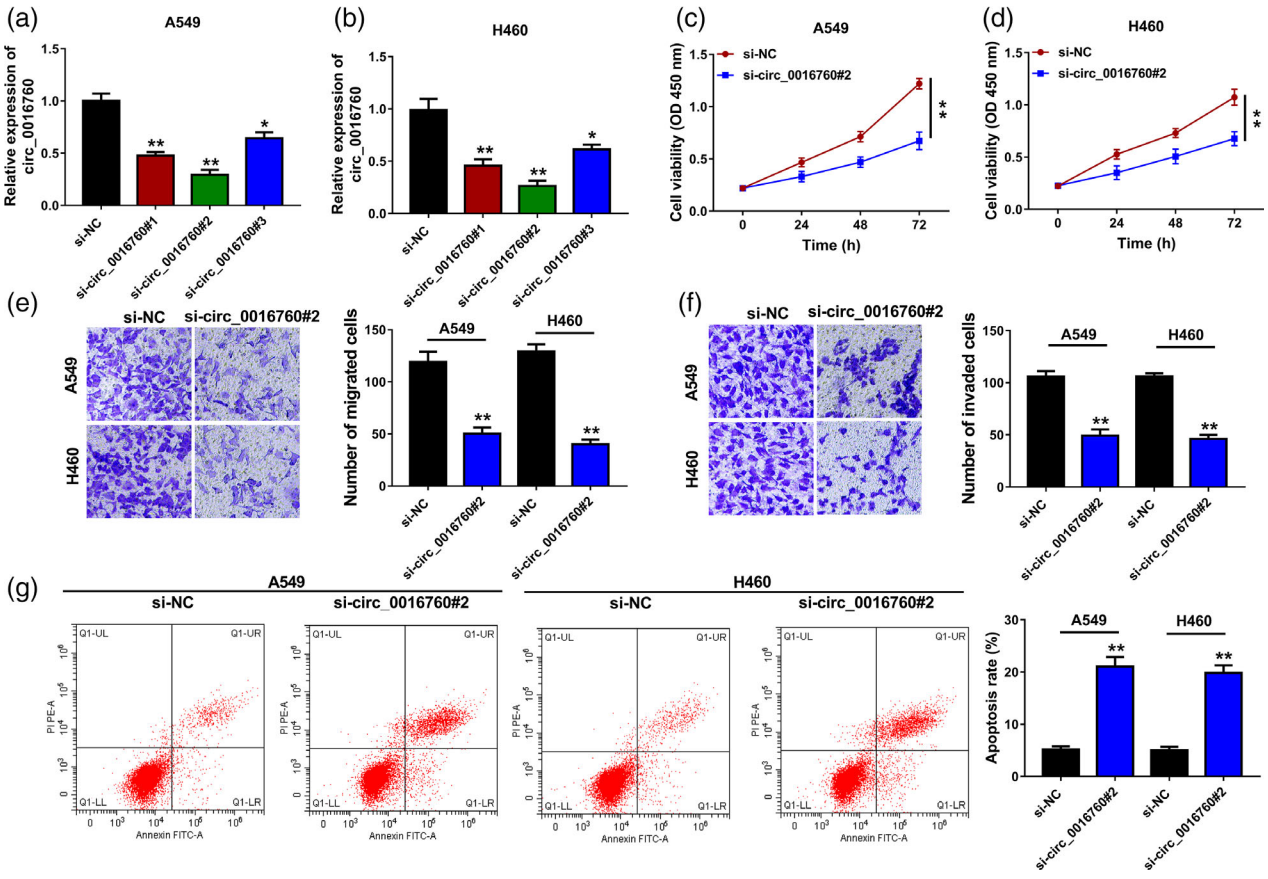

FIGURE 2 Circ_0016760 silencing hampers cell proliferation, migration, and invasion and triggers cell apoptosis in NSCLC cells. (a and b) The interference efficiencies of si-circ_0016760#1, si-circ_0016760#2, and si-circ_0016760#3 in NSCLC cells were assessed by qRT-PCR, and the si-NC-transfected group was used as the control group. (c–g) A549 and H460 cells were transfected with si-NC or si-circ_0016760#2. (c and d) CCK8 assay was conducted for the analysis of the cell proliferation curve in two groups. (e) Transwell migration assay was conducted to analyze cell migration ability after transfection for 24 h. (f) Cell invasion ability was analyzed through counting the number of invaded NSCLC cells via transwell invasion assay. (g) Flow cytometry was utilized to analyze cell apoptosis rates in two groups after 72 h of transfection. The apoptosis rate was analyzed as the percentages of NSCLC cells with $FITC^{+}$ and $PI^{+/-}$. $^{*}p < 0.05$, $^{**}p < 0.01$

the silencing of circ_0016760 (Figure 2c,d). Circ_0016760 interference notably reduced the numbers of migrated and invaded NSCLC cells (Figure 2e,f), suggesting that circ_0016760 depletion restrained cell migration and invasion abilities. Circ_0016760 interference also notably enhanced the apoptosis rate in two NSCLC cell lines (Figure 2g). These results suggested that circ_0016760 interference suppressed cell proliferation, migration, and invasion and induced the apoptosis of NSCLC cells.

MiR-646 is a target of circ_0016760 in NSCLC cells

Circular RNA Interactome software was used to predict the binding partners of circ_0016760, and miR-646 was predicted as a possible target of circ_0016760 (Figure 3a). Dual-luciferase reporter assay was conducted to verify the interaction between miR-646 and circ_0016760 and the binding sites. MiR-646 transfection dramatically decreased the luciferase activity with the co-transfection of WT-circ_0016760 compared with miR-NC and WT-circ_0016760 group (Figure 3b,c), suggesting the interaction between miR-646 and circ_0016760. Furthermore, luciferase activity in the MUT-circ_0016760 group remained unchanged with the co-transfection of miR-NC or miR-646 (Figure 3b,c), suggesting that "AGCUGCU" sites in circ_0016760 were indeed the target sites with miR-646. Circ_0016760 transfection significantly elevated its expression in NSCLC cells (Figure 3d). The MiR-646 level was reduced with the accumulation of circ_0016760, while circ_0016760 silencing increased the expression of miR-646 in NSCLC cells (Figure 3e,f), suggesting the negative

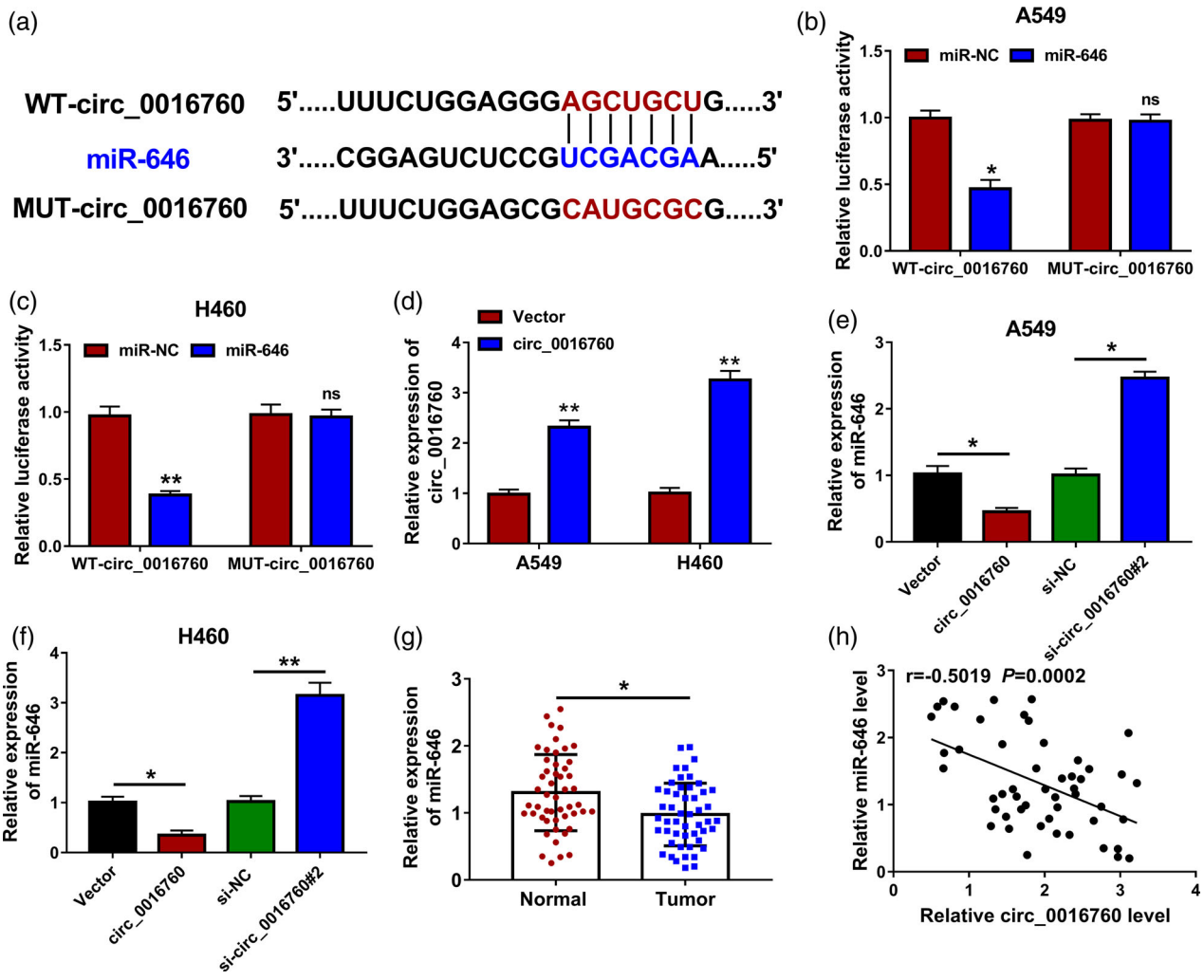

FIGURE 3 MiR-646 is a target of circ_0016760 in NSCLC cells. (a) The predicted binding sequence between miR-646 and circ_0016760 via Circular RNA Interactome software is shown. (b and c) A549 and H460 cells were co-transfected with miR-NC or miR-646 and WT-circ_0016760 or MUT-circ_0016760. Dual-luciferase reporter assay was used to analyze the luciferase activities in four groups to verify the interaction between miR-646 and circ_0016760. (d) The level of circ_0016760 was determined in NSCLC cells transfected with Vector or circ_0016760 for 24 h by qRT-PCR. (e and f) The expression of miR-646 was examined in A549 and H460 cells transfected with circ_0016760 or si-circ_0016760#2 along with their negative control (vector or si-NC) by qRT-PCR. (g) qRT-PCR was carried out for the examination of miR-646 expression in 50 pairs of NSCLC tissues and adjacent normal tissues. (h) The linear correlation between miR-646 and circ_0016760 was analyzed by Spearman's correlation coefficient. $^{*}p < 0.05$, $^{**}p < 0.01$; ns, no significant difference

regulatory relationship between miR-646 and circ_0016760 in NSCLC cells. Ago2 is an important component of the RNA-induced silencing complex (RISC), and it functions as a key regulator of microRNA functions.[25] Subsequently, we analyzed if the regulation of miR-646 by circ_0016760 was Ago2-dependent. High silencing efficiencies of two Ago2 siRNAs were confirmed by Western blot assay (Figure S2a). Circ_0016760 overexpression notably down-regulated the expression of miR-646 in NSCLC cells (Figure S2b,c). However, there was no significant difference in the expression of miR-646 in circ_0016760 plasmid and Ago2 siRNA co-transfected groups relative to their control groups (Figure S2b,c), demonstrating that the regulation of miR-646 by circ_0016760 was Ago2-dependent. There was a significant reduction in miR-646 expression in NSCLC tissues compared with that in adjacent normal tissues (Figure 3g). MiR-646 expression level was negatively correlated with the abundance of circ_0016760 (Figure 3h). Overall, circ_0016760 interacted with miR-646 and negatively regulated the expression of miR-646 in NSCLC cells.

Circ_0016760 interference-mediated effects are partly alleviated by the co-transfection with in-miR-646

The interference efficiency of in-miR-646 was high in NSCLC cells (Figure 4a). Si-circ_0016760#2 was co-transfected with in-miR-646 into NSCLC cells. Circ_0016760 interference enhanced the expression of miR-646, and the co-transfection with in-miR-646 decreased the level of miR-646 in NSCLC cells once again (Figure 4b,c). The circ_0016760 knockdown-mediated suppressive effect in cell proliferation was partly counteracted by the addition of in-miR-646 (Figure 4d, e), suggesting that circ_0016760 silencing restrained cell proliferation through enhancing the level of miR-646 in NSCLC cells. The number of migrated NSCLC cells was reduced with the silencing of circ_0016760, and cell migration ability was partly rescued with the introduction of in-miR-646 (Figure 4f). The number of invaded NSCLC cells in four groups exhibited a similar trend to the number of migrated NSCLC cells (Figure 4g), which together demonstrated that circ_0016760 knockdown

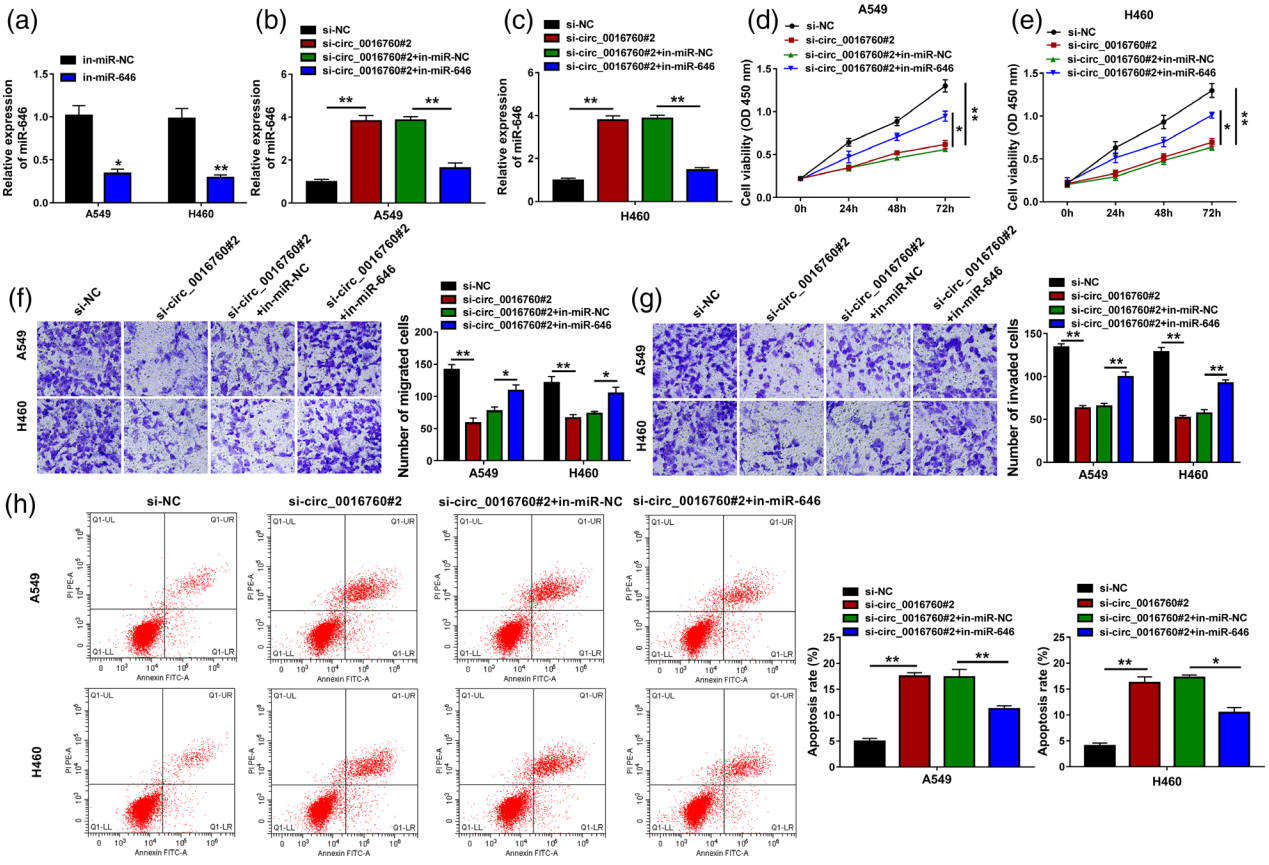

FIGURE 4 Circ_0016760 interference-mediated effects are partly alleviated by the co-transfection with in-miR-646. (a) The expression of miR-646 was determined in A549 and H460 cells transfected with in-miR-NC or in-miR-646 for 24 h via qRT-PCR. (b–h) A549 and H460 cells were transfected with si-circ_0016760#2 alone or together with in-miR-646. (b and c) qRT-PCR was applied to measure the level of miR-646 in NSCLC cells after transfection for 24 h. (d and e) The number of NSCLC cells after transfection for 0 h, 24 h, 48 h or 72 h was estimated via CCK8 assay, and the cell proliferation curve was generated. (f and g) The numbers of migrated and invaded NSCLC cells were assessed by transwell migration assay and transwell invasion assay. (H) Cell apoptosis rate was analyzed as the proportion of NSCLC cells with $FITC^+$ and $PI^{+/-}$ via flow cytometry. $^*p < 0.05$, $^{**}p < 0.01$

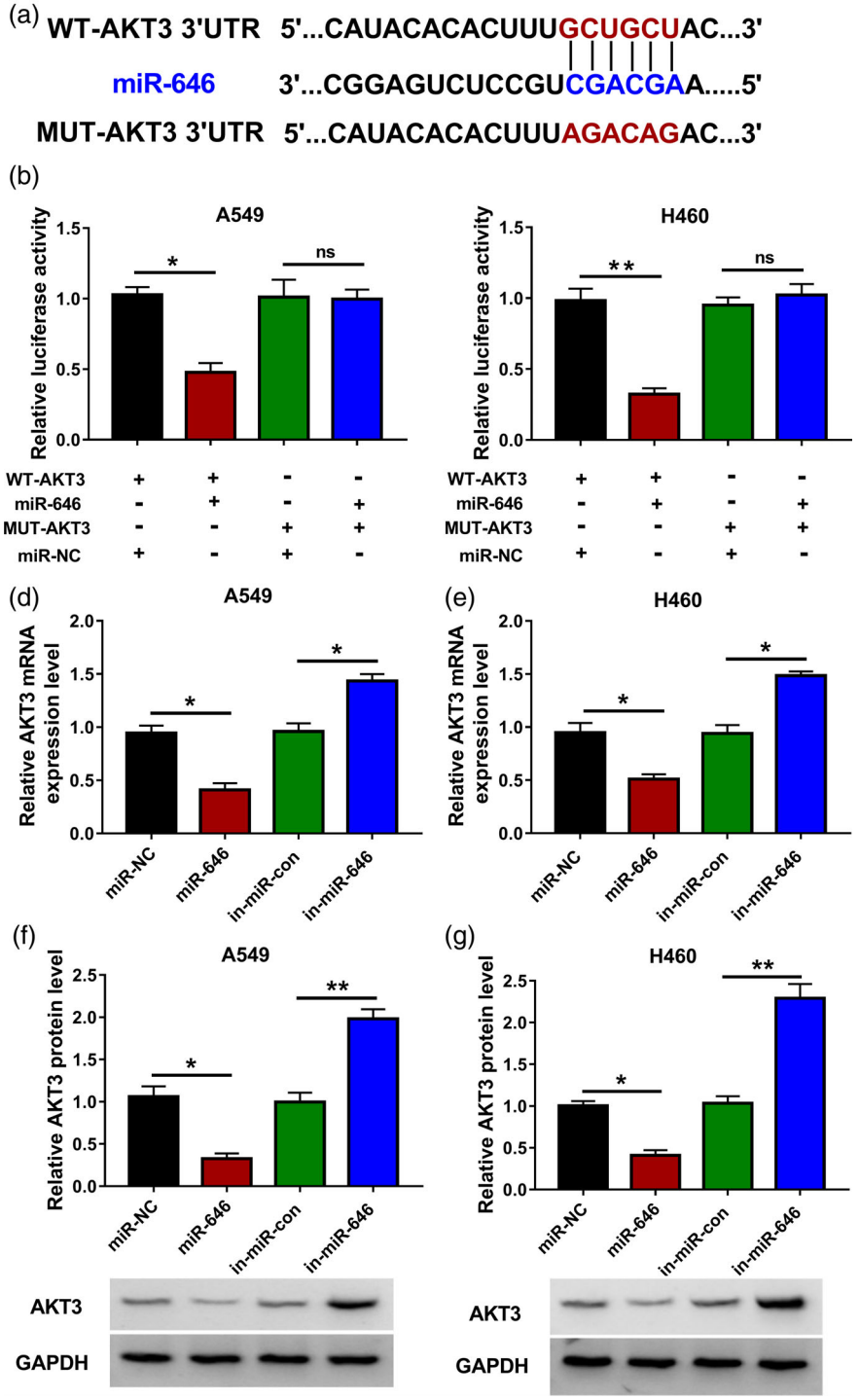

FIGURE 5 MiR-646 binds to AKT3 in NSCLC cells. (a) TargetScan software was used to predict the binding partners of miR-646, and the complementary sites between miR-646 and the 3′UTR of AKT3 are shown. (b and c) Dual-luciferase reporter assay was performed to confirm the target relationship between miR-646 and AKT3. (d and e) The mRNA level of AKT3 was examined in NSCLC cells transfected with miR-NC, miR-646, in-miR-NC or in-miR-646 via qRT-PCR. (f and g) Western blot assay was utilized for the determination of AKT3 protein expression in A549 and H460 cells transfected with miR-NC, miR-646, in-miR-NC or in-miR-646. $^{*}p < 0.05$, $^{**}p < 0.01$; ns, no significant difference

suppressed cell migration and invasion through upregulating miR-646. The cell apoptosis rate was elevated in the si-circ_0016760#2 group, and the addition of in-miR-646 inhibited the apoptosis of NSCLC cells (Figure 4h). Overall, circ_0016760 silencing-induced suppressive effects in cell proliferation, migration, and invasion, and promoting influence in cell apoptosis were all partly overturned by the silencing of miR-646.

MiR-646 binds to AKT3 in NSCLC cells

We predicted the downstream binding partners of miR-646 using the bioinformatics method via TargetScan software. As shown in Figure 5a, the sequence "GCUGCU" in the 3′ UTR of AKT3 was complementary with the sequence "CGACGA" in miR-646, thus AKT3 was predicted as one of the candidate targets of miR-646. The interaction between

miR-646 and AKT3 was subsequently confirmed by dual-luciferase reporter assay. As displayed in Figure 5b,c, the intensity of luciferase was declined with the co-transfection of miR-646 and WT-AKT3 relative to miR-NC and WT-AKT3 group, suggesting that miR-646 bound to AKT3 in NSCLC cells. Luciferase intensity was unaffected in the MUT-AKT3 group when co-transfected with miR-646 or miR-NC (Figure 5b,c), suggesting that AKT3 interacted with miR-646 via its "GCUGCU" sequence. Apart from AKT3, we also focused on the potential interactions between miR-646 and other members of the AKT family (AKT1 and AKT2). Through using the bioinformatics software TargetScan, AKT2 was also predicted to be a candidate target of miR-646, while there was no potential binding sequence between miR-646 and AKT1. The results of the dual-luciferase reporter assay revealed that miR-646 cannot interact with AKT2 in NSCLC cells (Figure S3). Thus we concentrated on the target interaction between miR-646 and AKT3 in the following experiments. We transfected miR-646 or in-miR-646 and their negative controls (miR-NC and in-miR-NC) into NSCLC cells to measure the expression of AKT3 to investigate the regulatory relationship between miR-646 and AKT3. MiR-646 accumulation caused significant reduction in both the mRNA and protein expression of AKT3 in NSCLC cells, while the mRNA and protein abundance of AKT3 was enhanced with the interference of miR-646 (Figure 5d–g). Taken

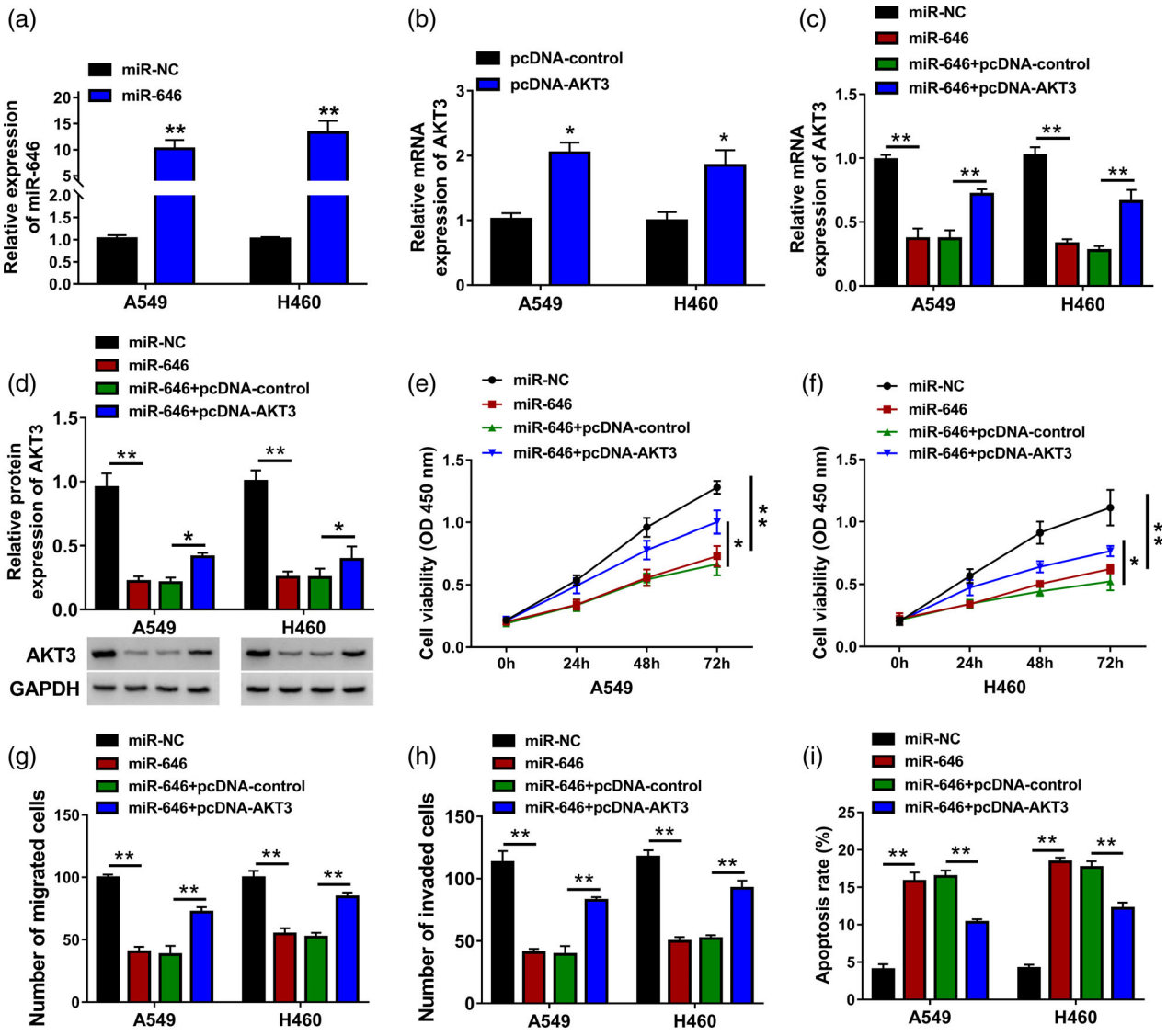

FIGURE 6 MiR-646 overexpression-induced effects in NSCLC cells are partly overturned by the accumulation of AKT3. (a) The overexpression efficiency of miR-646 was analyzed in NSCLC cells by qRT-PCR. (b) The expression of AKT3 mRNA was examined in A549 and H460 cells transfected with pcDNA-control or pcDNA-AKT3 by qRT-PCR. (C-I) A549 and H460 cells were transfected with miR-NC, miR-646, miR-646 + pcDNA-control or miR-646 + pcDNA-AKT3. (c) The mRNA expression of AKT3 was determined in transfected NSCLC cells by qRT-PCR. (d) The protein level of AKT3 was measured by Western blot assay. (e and f) CCK8 assay was used to analyze cell proliferation ability. (g and h) The migration and invasion abilities of NSCLC cells were analyzed by transwell migration and invasion assays. (i) Cell apoptosis rate was analyzed by flow cytometry, and the apoptosis rate indicated the apoptotic NSCLC cells with $FITC^{+}$ and $PI^{+/-}$. $^{*}p < 0.05$, $^{**}p < 0.01$

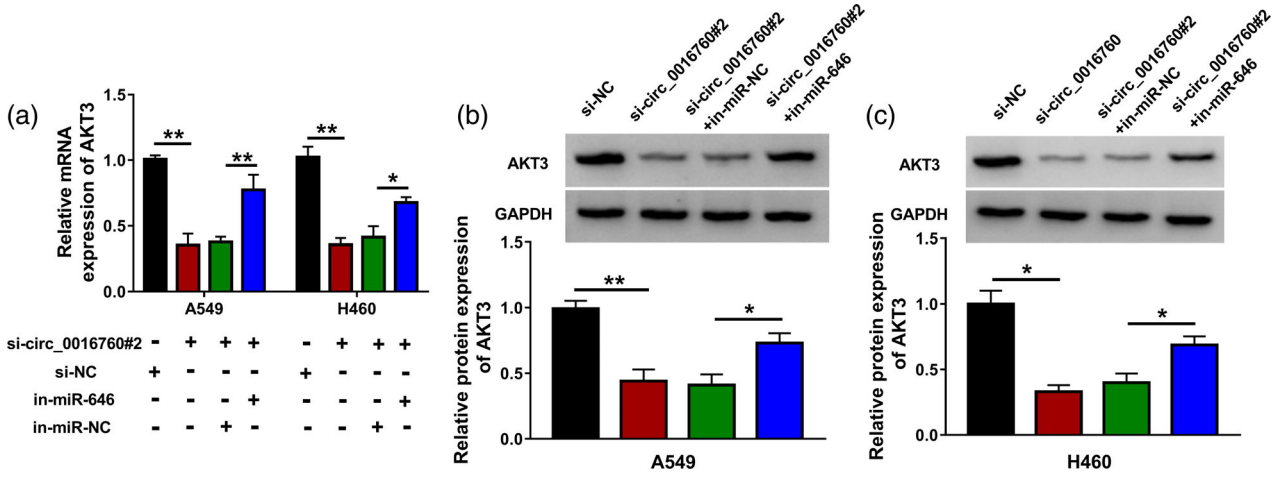

FIGURE 7 AKT3 is regulated by circ_0016760/miR-646 axis in NSCLC cells. (a–c) The mRNA and protein levels of AKT3 in A549 and H460 cells transfected with si-NC, si-circ_0016760#2, si-circ_0016760#2 + in-miR-NC or si-circ_0016760#2 + in-miR-646 were determined by qRT-PCR and Western blot assay. *$p < 0.05$, **$p < 0.01$

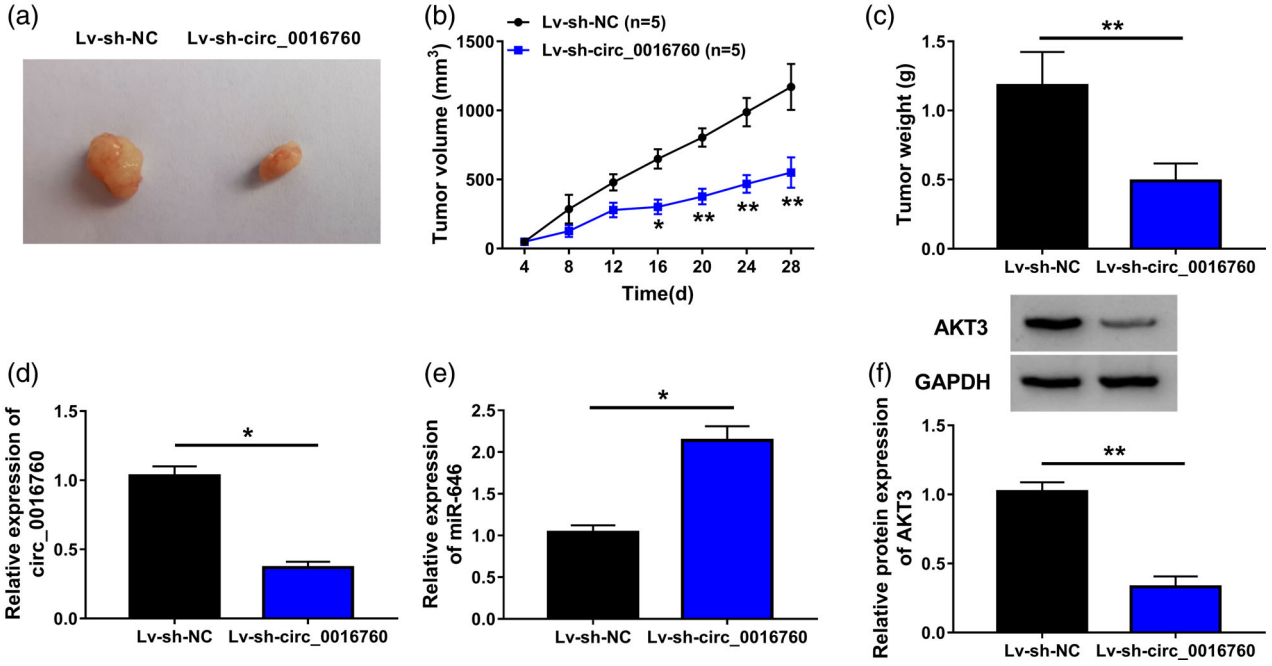

FIGURE 8 Circ_0016760 silencing blocks NSCLC progression in vivo. BALB/c mice were arbitrarily divided into two groups ($n = 5$). A total of 2.7×10^6 A549 cells stably expressing Lv-sh-NC or Lv-sh-circ_0016760 were subcutaneously injected into the mice. (a) The representative images of tumors in the Lv-sh-NC group and the Lv-sh-circ_0016760 group are shown. (b) Tumor volume was recorded every 4 days as length × width^2 × 0.5. (c) Tumors were weighed after 28 days of inoculation. (d and e) The expression of circ_0016760 and miR-646 was determined by qRT-PCR. (f) Western blot assay was implemented to measure the protein level of AKT3 in tumor tissues. *$p < 0.05$, **$p < 0.01$

together, AKT3 was confirmed as a target of miR-646, and it was negatively regulated by miR-646 in NSCLC cells.

MiR-646 overexpression-induced effects in NSCLC cells are partly overturned by the accumulation of AKT3

Loss-of-function experiments were conducted to explore the role of ATK3 in NSCLC cells. The high interference efficiency of si-AKT3 in NSCLC cells was verified by Western blot assay (Figure S4a). AKT3 silencing significantly restrained the proliferation, migration, and invasion, and induced the apoptosis of NSCLC cells (Figure S4b–f), suggesting that AKT3 exerted an oncogenic role in NSCLC cells. To investigate if miR-646-induced effects in NSCLC cells were partly based on its negative regulatory relationship with AKT3, we conducted compensation experiments through transfecting miR-646 alone or together with

pcDNA-AKT3 into NSCLC cells. We initially assessed the overexpression efficiencies of miR-646 mimics and pcDNA-AKT3 in NSCLC cells. MiR-646 mimics transfection notably increased the level of miR-646 in both A549 and H460 cells (Figure 6a). The transfection efficiency of pcDNA-AKT3 was high in NSCLC cells (Figure 6b). MiR-646 overexpression-induced reduction in AKT3 mRNA and protein expression was largely attenuated by the addition of pcDNA-AKT3 in NSCLC cells (Figure 6c,d). MiR-646 accumulation hampered cell proliferation, migration, and invasion while promoting the apoptosis of NSCLC cells (Figure 6e–i), and the tumor suppressor role of miR-646 was in agreement with the former results. As shown in Figure 6e,f, AKT3 overexpression partly rescued the proliferation ability of NSCLC cells which was restrained by the overexpression of miR-646. MiR-646 overexpression-induced suppression in cell migration and invasion was partly alleviated by the addition of pcDNA-AKT3 (Figure 6g,h). The accumulation of AKT3 also partly restrained miR-646-induced apoptosis in NSCLC cells (Figure 6I). Overall, miR-646 suppressed the proliferation, migration, and invasion and induced the apoptosis of NSCLC cells partly through reducing AKT3 expression.

AKT3 is regulated by circ_0016760/miR-646 axis in NSCLC cells

The above results suggest the negative regulatory interaction between miR-646 and circ_0016760 or AKT3, and we subsequently tested the regulatory interaction between circ_0016760 and AKT3 in NSCLC cells. Circ_0016760 knockdown reduced the mRNA and protein expression of AKT3, while this suppressive effect was partly counteracted by the addition of in-miR-646 in NSCLC cells (Figure 7a–c). These findings revealed that circ_0016760 enhanced the expression of AKT3 through sponging and downregulating miR-646 in NSCLC cells.

Circ_0016760 silencing blocks NSCLC progression in vivo

We further analyzed the role of circ_0016760 in the tumorigenicity of NSCLC tumors through xenograft tumor assay. Circ_0016760 silencing significantly restrained tumor growth of NSCLC in vivo (Figure 8a). Tumors from the Lv-sh-circ_0016760 group grew more slowly than that in the Lv-sh-NC group (Figure 8b). The tumors in the Lv-sh-NC group also had much heavier weight compared with that in the Lv-sh-circ_0016760 group (Figure 8c). Circ_0016760 expression was markedly reduced in the Lv-sh-circ_0016760 group in comparison with that in the Lv-sh-NC group (Figure 8d). Circ_0016760 knockdown notably enhanced the expression of miR-646 in tumor tissues (Figure 8e). Moreover, the AKT3 protein level was also found to be reduced with the silencing of circ_0016760 in tumor tissues (Figure 8f). The level of proliferation-associated marker Ki-67 in tumor tissues was also tested by immunohistochemistry. As shown in Figure S5, the Ki-67 level was notably reduced in tumor tissues in the Lv-sh-circ_0016760 group relative to the Lv-sh-NC group. Overall, these data demonstrate that circ_0016760 silencing suppressed NSCLC tumor growth in vivo.

DISCUSSION

Numerous circRNAs have been identified to be dysregulated in a variety of cancers, and the regulatory roles of circRNAs in cancers have also been documented.[26,27] As for NSCLC, Dong et al. claimed that circ_0076305 elevates the cisplatin resistance of NSCLC cells through targeting miR-296-5p/STAT3 axis.[28] Wang et al. proved that circ-PRMT5 contributes to the proliferation ability of NSCLC cells through elevating EZH2 expression via miR-377/miR-382/miR-498.[29] Li et al. claimed that circ_0016760 is highly expressed in NSCLC and high expression of circ_0016760 accelerates NSCLC progression via the miR-1287/GAGE1 signal axis. Hao et al. proved that circ_0016760 accelerates the colony formation, metastasis, and extracellular acidification rate of NSCLC cells to contribute to NSCLC progression via miR-577/ZBTB7A signaling.[30] Consistent with these reports, circ_0016760 abundance was significantly enhanced in NSCLC tissue specimens and cell lines. Circ_0016760 knockdown blocked cell proliferation, migration, and invasion while triggering the apoptosis of NSCLC cells.

After clarifying the role of circ_0016760 in NSCLC cells, we intended to elucidate the underlying mechanism behind the pro-tumor role of circ_0016760. It is generally known that circRNAs could act as miRNA sponges to release downstream mRNAs from the inhibition of miRNAs, thus elevating the expression of these mRNAs. For example, Sun et al. proved that circ-SFMBT2 accelerates the proliferation of gastric cancer cells through sponging miR-182-5p to elevate the enrichment of CREB1.[31] Tang et al. demonstrated that circ_0000515 facilitates the development of cervical cancer through upregulating ELK1 via sponging miR-326.[32] Here, the results of the dual-luciferase reporter assay verified that miR-646 bound to circ_0016760 in NSCLC cells. The negative regulatory relationship between miR-646 and circ_0016760 was then confirmed by qRT-PCR assay. Zhang et al. claimed that miR-646 hampers the proliferation and metastasis of gastric cancer cells through targeting FOXK1.[16] Li et al. reported that low abundance of miR-646 is associated with tumor metastasis in clear cell renal carcinoma.[33] MiR-646 suppresses the malignant progression of breast cancer through targeting HDAC2.[17] MiR-646 represses NSCLC development through targeting FGF2 and CCND2.[34] These works together demonstrate that miR-646 plays an antitumor role in cancers. MiR-646 abundance was reduced in NSCLC. The results of compensation experiments suggest that circ_0016760 silencing-mediated suppressive effects on the malignant properties of NSCLC cells are partly based on the upregulation of miR-646.

AKT3 was found to be a target of miR-646 in NSCLC cells. AKT3 is involved in tumorigenesis via PI3K/AKT signaling.[35,36] In addition, Li et al. found that AKT3 silencing

causes significant suppression in cell proliferation and motility in thyroid cancer cells.[37] Hu et al. demonstrated that AKT3 accelerates the proliferation and suppresses cell apoptosis of gastric cancer cells.[23] MiR-217 is found to attenuate the progression of NSCLC through suppressing AKT3.[24] We found that AKT3 was negatively modulated by miR-646, and miR-646 overexpression restrained NSCLC progression through reducing AKT3. Circ_0016760 positively regulated AKT3 expression through sponging miR-646 in NSCLC cells. The results of xenograft tumor assay suggested that circ_0016760 knockdown notably blocked the tumor growth of NSCLC in vivo.

In summary, miR-646 was confirmed as a target of circ_0016760, and AKT3 was verified as a target of miR-646 in NSCLC cells. Circ_0016760 contributed to the proliferation and metastasis, and restrained cell apoptosis of NSCLC cells through targeting the miR-646/AKT3 axis, which provided new insight into developing novel therapeutic methods for NSCLC patients. Circ_0016760 and AKT3 might be effective therapeutic targets in NSCLC treatment, and restoration of miR-646 expression might be a potential therapeutic strategy for NSCLC patients.

CONFLICT OF INTEREST

The authors declare that there are no competing interests associated with the manuscript.

ORCID

Yanli Cai https://orcid.org/0000-0002-0181-8248

REFERENCES

1. Friedlaender A, Addeo A, Russo A, Gregorc V, Cortinovis D, Rolfo CD. Targeted therapies in early stage NSCLC: hype or hope? Int J Mol Sci. 2020;21(17):6329.
2. Willers H, Azzoli CG, Santivasi WL, Xia F. Basic mechanisms of therapeutic resistance to radiation and chemotherapy in lung cancer. Cancer J. 2013;19(3):200–7.
3. Verdecchia A, Francisci S, Brenner H, Gatta G, Micheli A, Mangone L, et al. Recent cancer survival in Europe: a 2000-02 period analysis of EUROCARE-4 data. Lancet Oncol. 2007;8(9):784–96.
4. Lan D, Zhang X, He R, Tang R, Li P, He Q, et al. MiR-133a is down-regulated in non-small cell lung cancer: a study of clinical significance. Eur J Med Res. 2015;20(1):50.
5. Li Y, Zheng Q, Bao C, Li S, Guo W, Zhao J, et al. Circular RNA is enriched and stable in exosomes: a promising biomarker for cancer diagnosis. Cell Res. 2015;25(8):981–4.
6. Salzman J, Circular RNA. Expression: its potential regulation and function. Trends Genet. 2016;32(5):309–16.
7. Du WW, Yang W, Li X, Awan FM, Yang Z, Fang L, et al. A circular RNA circ-DNMT1 enhances breast cancer progression by activating autophagy. Oncogene. 2018;37(44):5829–42.
8. Shen T, Cheng X, Liu X, Xia C, Zhang H, Pan D, et al. Circ_0026344 restrains metastasis of human colorectal cancer cells via miR-183. Artif Cells Nanomed Biotechnol. 2019;47(1):4038–45.
9. Li Y, Hu J, Li L, Cai S, Zhang H, Zhu X, et al. Upregulated circular RNA circ_0016760 indicates unfavorable prognosis in NSCLC and promotes cell progression through miR-1287/GAGE1 axis. Biochem Biophys Res Commun. 2018;503(3):2089–94.
10. Saliminejad K, Khorram Khorshid HR, Soleymani Fard S, Ghaffari SH. An overview of microRNAs: biology, functions, therapeutics, and analysis methods. J Cell Physiol. 2019;234(5):5451–65.
11. Ali Syeda Z, Langden SS, Munkhzul C, Lee M, Song SJ. Regulatory mechanism of microRNA expression in cancer. Int J Mol Sci. 2020;21(5):1723.
12. Liu B, Shyr Y, Cai J, Liu Q. Interplay between miRNAs and host genes and their role in cancer. Brief Funct Genomics. 2018;18(4):255–66.
13. Han B, Chao J, Yao H. Circular RNA and its mechanisms in disease: from the bench to the clinic. Pharmacol Ther. 2018;187:31–44.
14. Liang HF, Zhang XZ, Liu BG, Jia GT, Li WL. Circular RNA circ-ABCB10 promotes breast cancer proliferation and progression through sponging miR-1271. Am J Cancer Res. 2017;7(7):1566–76.
15. Chen T, Yang Z, Liu C, Wang L, Yang J, Chen L, et al. Circ_0078767 suppresses non-small-cell lung cancer by protecting RASSF1A expression via sponging miR-330-3p. Cell Prolif. 2019;52(2):e12548.
16. Zhang P, Tang WM, Zhang H, Li YQ, Peng Y, Wang J, et al. MiR-646 inhibited cell proliferation and EMT-induced metastasis by targeting FOXK1 in gastric cancer. Br J Cancer. 2017;117(4):525–34.
17. Darvishi N, Rahimi K, Mansouri K, Fathi F, Menbari MN, Mohammadi G, et al. MiR-646 prevents proliferation and progression of human breast cancer cell lines by suppressing HDAC2 expression. Mol Cell Probes. 2020;101649:101649.
18. Pan Y, Chen Y, Ma D, Ji Z, Cao F, Chen Z, et al. miR-646 is a key negative regulator of EGFR pathway in lung cancer. Exp Lung Res. 2016;42(6):286–95.
19. Zhang Y, Shi Z, Li Z, Wang X, Zheng P, Li H. Circ_0057553/miR-515-5p regulates prostate cancer cell proliferation, apoptosis, migration, invasion and aerobic glycolysis by targeting YES1. Onco Targets Ther. 2020;13:11289–99.
20. Fabian MR, Sonenberg N, Filipowicz W. Regulation of mRNA translation and stability by microRNAs. Annu Rev Biochem. 2010;79:351–79.
21. Guo H, Ingolia NT, Weissman JS, Bartel DP. Mammalian microRNAs predominantly act to decrease target mRNA levels. Nature. 2010;466(7308):835–40.
22. Ruan L, Qian X. MiR-16-5p inhibits breast cancer by reducing AKT3 to restrain NF-κB pathway. Biosci Rep. 2019;39(8):BSR20191611.
23. Hu J, Ni G, Mao L, Xue X, Zhang J, Wu W, et al. LINC00565 promotes proliferation and inhibits apoptosis of gastric cancer by targeting miR-665/AKT3 axis. Onco Targets Ther. 2019;12:7865–75.
24. Qi YJ, Zha WJ, Zhang W. MicroRNA-217 alleviates development of non-small cell lung cancer by inhibiting AKT3 via PI3K pathway. Eur Rev Med Pharmacol Sci. 2018;22(18):5972–9.
25. Ye Z, Jin H, Qian Q. Argonaute 2: a novel rising star in cancer research. J Cancer. 2015;6(9):877–82.
26. Zhang HD, Jiang LH, Sun DW, Hou JC, Ji ZL. CircRNA: a novel type of biomarker for cancer. Breast Cancer. 2018;25(1):1–7.
27. Meng S, Zhou H, Feng Z, Xu Z, Tang Y, Li P, et al. CircRNA: functions and properties of a novel potential biomarker for cancer. Mol Cancer. 2017;16(1):94.
28. Dong Y, Xu T, Zhong S, Wang B, Zhang H, Wang X, et al. Circ_0076305 regulates cisplatin resistance of non-small cell lung cancer via positively modulating STAT3 by sponging miR-296-5p. Life Sci. 2019;239:116984.
29. Wang Y, Li Y, He H, Wang F. Circular RNA circ-PRMT5 facilitates non-small cell lung cancer proliferation through upregulating EZH2 via sponging miR-377/382/498. Gene. 2019;720:144099.
30. Hao Y, Xi J, Peng Y, Bian B, Hao G, Xi Y, et al. Circular RNA Circ_0016760 modulates non-small-cell lung cancer growth through the miR-577/ZBTB7A Axis. Cancer Manag Res. 2020;12:5561–74.
31. Sun H, Xi P, Sun Z, Wang Q, Zhu B, Zhou J, et al. Circ-SFMBT2 promotes the proliferation of gastric cancer cells through sponging miR-182-5p to enhance CREB1 expression. Cancer Manag Res. 2018;10:5725–34.
32. Tang Q, Chen Z, Zhao L, Xu H. Circular RNA hsa_circ_0000515 acts as a miR-326 sponge to promote cervical cancer progression through up-regulation of ELK1. Aging (Albany NY). 2019;11(22):9982–99.
33. Li W, Liu M, Feng Y, Xu YF, Huang YF, Che JP, et al. Downregulated miR-646 in clear cell renal carcinoma correlated with tumour metastasis by targeting the nin one binding protein (NOB1). Br J Cancer. 2014;111(6):1188–200.

34. Wang J, Shu H, Guo S. MiR-646 suppresses proliferation and metastasis of non-small cell lung cancer by repressing FGF2 and CCND2. Cancer Med. 2020;9(12):4360–70.
35. Bellacosa A, Kumar CC, Di Cristofano A, Testa JR. Activation of AKT kinases in cancer: implications for therapeutic targeting. Adv Cancer Res. 2005;94:29–86.
36. Paul-Samojedny M, Pudełko A, Kowalczyk M, Fila-Daniłow A, Suchanek-Raif R, Borkowska P, et al. Combination therapy with AKT3 and PI3KCA siRNA enhances the antitumor effect of temozolomide and carmustine in T98G glioblastoma multiforme cells. BioDrugs. 2016;30(2):129–44.
37. Li R, Liu J, Li Q, Chen G, Yu X. miR-29a suppresses growth and metastasis in papillary thyroid carcinoma by targeting AKT3. Tumour Biol. 2016;37(3):3987–96.

SUPPORTING INFORMATION

Additional supporting information may be found in the online version of the article at the publisher's website.

How to cite this article: Chen S, Zhou L, Ran R, Huang J, Zheng Y, Xing M, et al. Circ_0016760 accelerates non-small-cell lung cancer progression through miR-646/AKT3 signaling in vivo and in vitro. Thorac Cancer. 2021;12:3223–35. https://doi.org/10.1111/1759-7714.14191